The Unified Power Flow Controller: A possible solution to support wind energy penetration in the power system

H. Brahmi ,R. Dhifaoui

Abstract – *Improving power systems transfer capability, voltage level control, damping electromechanical power oscillations and reducing transient swings becomes a great concern for national and/or private energy companies. Around the word, in particular in emerging countries, energy demand is in very fast growth. Developments of conventional and renewable energy production sources follow closely such fast increase in energy absorption. But, in general, developments in transmission lines and in hard and software control equipments are well delayed which implies a dangerous gap between the demand and the transmission capacity. Failures can give rise to power oscillation, voltage drop and high frequency deviations; resulting in system integrity rapid collapse by transient stability mechanism. New technology alternatives as FACTS can positively support conventional control systems as PSSs, AVRs and TGs .The paper deals with this problem and aims to show that UPFC is a suitable device in particular to reinforce variable wind energy penetration in the power system.*

Keywords: *Power systems, Transfer capability, Voltage control, Wind energy, Unified power flow controller, Injection model*

Nomenclature

FACTS: Flexible Alternating Current Transmission Systems

PSS: Power System Stabilizer

AVR: Automatic Voltage Regulator

TG: Turbine Governor

UPFC: Unified Power Flow Controller

SVC: Static Var Compensator

TSCS: Thyristor Controlled Series Capacitor

DAE: Differential and Algebraic Equations

PSAT: Power System Analysis Toolbox

I. Introduction

Around the word, in particular in emerging countries, energy demand is in very fast growth. Developments of energy production sources follow closely such fast increase in energy absorption. But, in general, developments in transmission lines and in hard and software control equipments are well delayed which implies a dangerous gap between the demand and the transmission capacity. In fact, it was proved that a great part of failures that have severely tricked large scale power networks are related to insufficient transfer capability and inadequate or absent control processes. Failures can give rise to power oscillation, voltage drop and high frequency deviations; resulting in system integrity rapid collapse by transient stability mechanism. Furthermore, transients in power systems are today more excited by the presence of wind energy sources. Such energy is by nature variable with wind speed that is variable with geography. Consequently, improving power systems transfer capability, damping electromechanical power oscillations and reducing transient swings of system variables becomes a great concern for national and/or private energy companies. For reasons listed before, conventional control systems as PSSs, AVRs and TGs are insufficient for modern power networks. This has been in reality observed more then 20 years ago and some promising alternatives well known as FACTS have been proposed [1]-[2]. The most attractive solution is labelled UPFC [3]-[4].

UPFC has the ability to adjust simultaneously the bus voltage magnitude, the transmission line reactance and the transited power or current flow. Therefore, all classic solutions of shunt as SVC and series as TSCS compensation processes are present in the UPFC [5] - [6] [7]. The general configuration of this system is shown by Fig.1.

Manuscript received November 2008, revised December2008

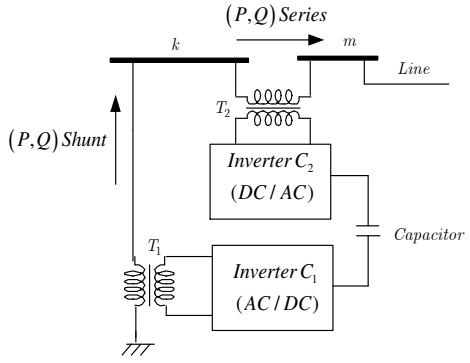

Fig.1. General structure of an UPFC

The UPFC has a shunt transformer T1 driven from the bus and a series transformer T2 injected in the line. These two transformers are coupled by two inverters that are separated by a DC link. The capacitor is controlled so that some active power quantity is extracted by inverter C1 from the bus and injected by inverter C2 in the transmission line via transformer T2. In terms of reactive power, the control is more flexible in the sense that inverter 1 can works as generator as well as receiver. Through the series part, the reactive power balance is also relatively easy to establish.

Basic potentialities of UPFC are proved and largely demonstrated via various mathematical modelling approaches presented in the literature [8 to 12]. However, one can note that the proposed models treat always the two parts separately in one hand and largely simplify their dynamics on the other hand. Taking into account all local variables and practical dimensional constraints for example is not well studied.

Three principal topics cover the study summarized in this paper. First, we believe that it very useful to present the theory of the injection model of the UPFC and bring out in the best possible way the mechanism of energy transit between the two branches of the device. Second, our aim is to present a simple but reliable control scheme that ensures a suitable convergence to a very adequate steady state operating point. Beside this, a validation stage by simulation of the UPFC response in presence of a power system is needed. To discover the real capabilities of the device, tests in worst cases of operating are required. It is for this reason that we have considered the case of wind energy.

Thus, we present in section 2 the dynamical model of the synchronous machine conjointly with transmission power system algebraic state. Then, in section 3, we briefly introduce the model of the wind energy source. The great developments will be presented in section 4 that deals with the injection model of the UPFC. The power balance of the system is investigated and all necessary equations to introduce the principle of power injection model are presented and commented. PQ generators are then defined to describe the UPFC device. The control of these generators is presented and discussed in section 5. Finally, section 6 is reserved to illustration. All the necessary data of the power system under study are given. A perturbation scenario is simulated and the results are commented.

II. Synchronous machine model

Generally speaking, power system dynamics are described by a mathematical model composed by DAE [13] as indicated by equations (1) and (2).

$$\begin{cases} \dfrac{dx}{dt} = f(x, y, p(t)) & (1) \\ 0 = g(x, y, p(t)) & (2) \end{cases}$$

The function $g(x, y, p(t))$ corresponds to Ohm's and Kirchoff's equations of the circuit where voltage magnitudes and phases are illustrated by the algebraic variables y .Variables x ,governed by the function $f(x, y, p(t))$, are associated to the systems state variables and include for example synchronous machine speed and transient emfs. They also include control variables as those of TGs and AVRs variables. Variable $p(t)$ can model an external perturbation parameter introduced for particular topic. These DAEs are basically solved by a trapezoidal Newton-Raphson based technique with possible variable integration step.

In the system that will be studied, synchronous machines are described by a fourth order model limited to dynamics of rotor angle, machine speed and direct and quadrature components of the internal transient emf. No classical control is here considered to observe only the effect of the UPFC device. Machine emf and terminal current and voltage are expressed in a synchronously rotating reference frame linked to a selected slack bus. We use here conventional notations and refer the reader to related literature and to [14] in particular.

In this context, mechanical motion of the synchronous machine is expressed by differential equations (3) and (4) where P_M and P_G hold respectively for the input mechanical power and the output electric power. The parameters ω_b , H and D define respectively the base frequency of the power system, inertia time constant and damping coefficient of the synchronous generator. Variable ω_r is the per unit machine speed. Dynamics behaviour of machine transient emf are given by equation (5) and (6) characterizing the flux decay phenomenon. Voltage and current components, machine active power P_G and reactive power Q_G are given by algebraic equations (7) to (11).

$$\begin{cases} \dfrac{d\delta_r}{dt} = \omega_b(\omega_r - 1) & (3) \\ \dfrac{d\dot{\omega}_r}{dt} = \dfrac{P_M - D(\omega_r - 1) - P_G}{2H} & (4) \\ \dfrac{dE_d^{'}}{dt} = \dfrac{-E_d^{'} + (X_q - X_q^{'})I_q}{T_{qo}^{'}} & (5) \\ \dfrac{d\dot{E}_q^{'}}{dt} = \dfrac{E_{fd} - E_q^{'} - (X_d - X_d^{'})I_d}{T_{do}^{'}} & (6) \end{cases}$$

$$\begin{cases} E_d^{'} - R_s I_d + X_q^{'} I_q - V_d = 0 & (7) \\ E_q^{'} - X_d^{'} I_d - R_s I_q - V_q = 0 & (8) \\ V_d I_d + V_q I_q - P_G = 0 & (9) \\ P_G - E_d^{'} I_d - E_q^{'} I_q - (X_d^{'} - X_q^{'}) I_d I_q = 0 & (10) \\ Q_G - E_q^{'} I_d + E_d^{'} I_q + X_d^{'} I_q^{\,2} + X_q^{'} I_d^{\,2} = 0 & (11) \end{cases}$$

It is to note that as mentioned above, mechanical power P_M and direct field voltage E_{fd} are kept constant during transient. Note also that this model is written for every synchronous machine i present the power system. Therefore, these equations are to be added to power balance equations at machine terminal bus as follows.

$$\begin{cases} P_G + p(t) - P_{Load} - \sum PLines = 0 & (12) \\ Q_G - Q_{Load} - \sum QLines = 0 & (13) \end{cases}$$

III. Wind energy source model

As the principal targeted goal is here the UPFC device study, we will consider a simplified model for wind energy sources. Detailed models can be found in the literature [15 to 18] and our previous works [19] [20]. Let us recall that available wind energy generators around the world are in great part standard squirrel cage and doubly fed asynchronous machines.

For these machines, active power is expressed in terms of a rotor resistance variable versus machine sleep frequency. So for simplicity, we represent these generators as sketched by Fig.2 where parameters $\bar{z}_w$ and jX_w illustrate rotor transient impedance and stator magnetizing reactance. The stator transient impedance can be included in the transmission line connected to the generator. Energy extracted from the wind is characterized by a variable active power injection $p(t)$. The frequency adaptation problem is assumed realized by fast and ideal invertors. The variable $p(t)$ is taken dynamically slow as compared to the power system variables. This assumption permits to consider $p(t)$ constant during the integration step used while solving DAEs. We obtain consequently a sufficiently stable integration process. The active power injection $p(t)$ is added step by step to buses power balance.

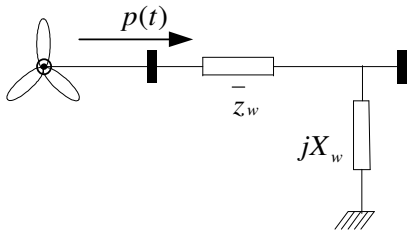

Fig.2. The wind energy generator model

IV. The power injection model of the UPFC

First, let us indicate by k and m respectively the input bus and the output bus between them the UPFC is placed. We note by jx_T the transformer reactance of the series part of the UPFC device. As the main function of the series branch of the UPFC is to inject in the transmission line an AC voltage with controllable magnitude and phase, we consider an ideal series voltage source $\bar{v}_T$ delivering to the receiving bus m the current $\bar{I}_{km}$ through the reactance jx_T. The shunt branch is driven from bus k and has the function to inject active power P_{sh} and reactive power Q_{sh} quantities. In this point of view, we consider Fig.3 to illustrate this model widely used in literature.

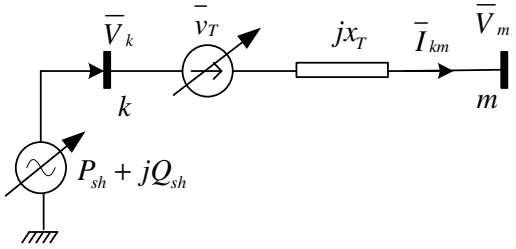

Fig.3. The physical model of the UPFC

Implementation of this model conjointly with available software packages presents serious difficulties. In fact, power systems simulation programs are based on only shunt energy sources where zero voltage is linked to ground point. Thus, including series energy sources in these packages requires fundamental transformations. To overcome this problem, a solution based on equivalent power injection model is proposed [9]. In the sense of this solution, we consider the equivalent model described by Fig.4 and we give necessary developments to establish values of P_k, Q_k, P_m and Q_m.

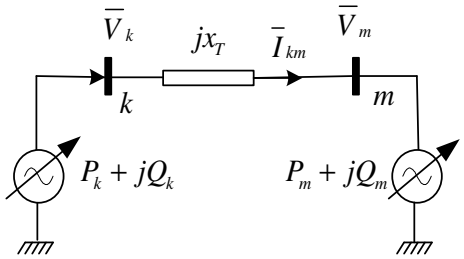

Fig.4. The injection equivalent model of the UPFC

Let $\overline{V}_k = V_k e^{j\theta_k}$ and $\overline{V}_m = V_m e^{j\theta_m}$ be the voltage vectors of the input port and output port respectively. Angles θ_k and θ_m are computed with respect to the slack bus reference frame rotating at the fundamental frequency. The series branch is governed by the two equivalent following equations:

$$\overline{V}_k + \overline{v}_T = jx_T \overline{I}_{km} + \overline{V}_m \tag{14}$$

$$\overline{I}_{km} = -jb_T \overline{v}_T - jb_T(\overline{V}_k - \overline{V}_m) \quad b_T = 1/x_T \tag{15}$$

In the sense of the duality principle between Thevenin's voltage source and Norton's current source, the series part of Fig.3 can be replaced by the equivalent circuit of Fig.5. Thus, we have a current generator $\overline{i}_T = -jb_T \overline{v}_T$ in parallel with admittance $-jb_T$ of the transformer. This current source $\overline{i}_T$ produces at ports k and m two injected power quantities defined as follows:

$$\overline{s}_{Ik} = P_{Ik} + jQ_{Ik} = \overline{V}_k \overline{i}_T^{\,*} \tag{16}$$

$$\overline{s}_{\mathrm{Im}} = P_{\mathrm{Im}} + jQ_{\mathrm{Im}} = -\overline{V}_m \overline{i}_T^{\,*} \tag{17}$$

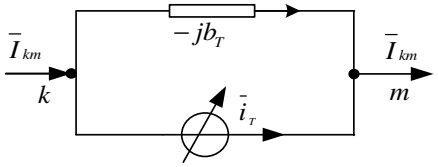

Fig.5. Parallel Norton's equivalent current

Using this equivalence solves computation of the different injection powers of equivalent UPFC circuit given by Fig.4. Without loss of generality but for more convenient mathematical formulation, we consider that series voltage source $\overline{v}_T$ has an angle γ with respect to a reference frame transported by the voltage vector $\overline{V}_k$ of the input bus k as indicated by Fig.6. Consequently, with respect to the reference bus bar of the network, $\overline{v}_T$ is expressed as $\overline{v}_T = v_T e^{j(\theta_k + \gamma)}$ and in the reference frame of $\overline{V}_k$ it is noted $\overline{v}_T = v_T e^{j\gamma} = v_{TD} + jv_{TQ}$. In the remaining part of the paper we consider this frame of work and we set:

$$\overline{v}_T = v_{TD} + jv_{TQ} = v_T(\cos\gamma + j\sin\gamma) \tag{18}$$

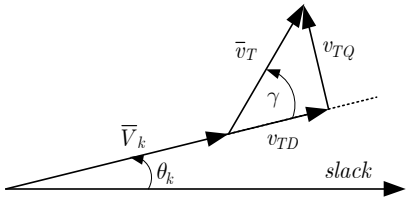

Fig.6 .Definition of the series voltage source vector

Thus, Norton's current-power equivalence gives rise to the following equations:

$$\overline{s}_{Ik} = b_T V_k (v_{TQ} + jv_{TD}) \tag{17}$$

$$\overline{s}_{\mathrm{Im}} = -b_T V_m (v_{TQ} + jv_{TD}) e^{-j(\theta_k - \theta_m)} \tag{18}$$

Separating real part from imaginary one gives:

$$P_{Ik} = b_T V_k v_{TQ} \tag{19}$$

$$Q_{Ik} = b_T V_k v_{TD} \tag{20}$$

$$P_{\mathrm{Im}} = -b_T V_m (v_{TQ}\cos\theta_{km} + v_{TD}\sin\theta_{km}) \tag{21}$$

$$Q_{\mathrm{Im}} = -b_T V_m (v_{TD}\cos\theta_{km} - v_{TQ}\sin\theta_{km}) \tag{22}$$

$$\theta_{km} = \theta_k - \theta_m \tag{23}$$

The series voltage source $\overline{v}_T$ supplies apparent complex power defined by:

$$\overline{S}_V = P_V + jQ_V = \overline{v}_T \overline{I}_{km}^{\,*} \tag{24}$$

$$P_V = b_T V_m (v_{TD}\sin\theta_{km} + v_{TQ}\cos\theta_{km}) - b_T v_{TQ} V_k \tag{25}$$

$$Q_V = b_T V_m (v_{TQ}\sin\theta_{km} - v_{TD}\cos\theta_{km}) + b_T (v_{TD} V_k + {v_T}^2) \tag{26}$$

Assuming that the UPFC structure is lossless and with respect to the actual circuit of Fig.3, active power control should impose $P_{sh} = P_V$. So to pass to the virtual equivalent circuit of Fig4, we state:

$$P_k = P_{sh} + P_{Ik} = P_V + P_{Ik} \tag{27}$$

$$P_m = P_{\mathrm{Im}} \tag{28}$$

Reactive power control of the shunt branch is realized independently of that of active power. So, in similar

way, the reactive power equivalence between Fig.3 and Fig.4 implies:

$$Q_k = Q_{sh} + Q_{Ik} = Q_{sh} + Q_{Ik} \quad (29)$$

$$Q_m = Q_{\mathrm{Im}} \quad (30)$$

Input and output active and reactive power injections of the equivalent model described by Fig.4 are finally governed by:

$$P_k = b_T \left(v_{TD} V_m \sin\theta_{km} + v_{TQ} V_m \cos\theta_{km} \right) \quad (31)$$

$$P_m = -P_k \quad (32)$$

$$Q_k = Q_{sh} + b_T v_{TD} V_k \quad (33)$$

$$Q_m = b_T V_m (v_{TQ} \sin\theta_{km} - v_{TD} \cos\theta_{km}) \quad (34)$$

Note finally that the output port of the UPFC supplies a transmission line. The previous developments naturally hold if we integrate the reactance of the line in the reactance of the transformer.

V. The considered UPFC control strategy

Surely, the most important raison of using UPFC is to enhance the power transfer capability of the associate transport line. The transported active power by a lossless line, as the case previously considered, is defined by: $P_{km} = b_T V_k V_m \sin\theta_{km}$ (35)

For a regulated voltage, the maximum power flow through the line varies in opposite sense with the line reactance. Thus, a well known solution to enhance transfer power capability is to reduce this reactance. Decreasing x_T decreases also voltage angle difference between the two buses and can ensure a positive reaction on transient stability phenomenon. Fixed capacitor or variable capacitor with switched thyristor lies in this solution. This function can be also realized by UPFC if we impose to it to establish a compensation ratio η_x of the transport line reactance. Let us first consider simple control laws such as those indicated by equations (36) and (37) to command the components of the series voltage source of the UPFC.

$$\frac{dv_{TQ}}{dt} = \frac{\upsilon_{TQ}^{ref} - v_{TQ}}{\tau_V} \quad (36)$$

$$\frac{dv_{TD}}{dt} = \frac{\upsilon_{TD}^{ref} - v_{TD}}{\tau_V} \quad (37)$$

To be sure that the UPFC emulates a capacitor, the components of the series voltage source should be linked to those of the transported current by the following equalities.

$$\upsilon_{TD}^{ref} = -\eta_x x_T I_Q \quad (38)$$

$$\upsilon_{TQ}^{ref} = \eta_x x_T I_D \quad (39)$$

Note that all components are reported in the reference frame of the input port voltage. The reference values being taken variable with the current line, the UPFC will have an internal constant reactance. On the other hand, components of the series voltage should respect dimensional limits. We impose therefore to dynamics of these components to respect the following constraints of upper and lower limits.

$$v_{\min} \le v_{TD} \le v_{\max} \quad (40)$$

$$-\sqrt{{v_{\max}}^2 - {v_{TD}}^2} \le v_{TQ} \le \sqrt{{v_{\max}}^2 - {v_{TD}}^2} \quad (41)$$

Furthermore, it is important not only to consider voltage limits but also to take into account reasonable limit on the power flow. The active power that departs from the input port to the output port is given by:

$$P_{km} = b_T V_k V_m \sin\theta_{km} + b_T V_k v_{TQ} \quad (42)$$

This equation shows that the presence of the UPFC introduces a power deviation ΔP (the second right term) with respect to the base case without this device (the first right term). In this study, we consider a limitation ratio η_p :

$$\left| \frac{\Delta P}{P_{km} - \Delta P} \right| \le \eta_p \quad (43)$$

This returns to consider the following constraint on the quadrature component of the series injected voltage source. This new constraint is treated simultaneously with constraints (40) and (41).

$$-V_m |\sin\theta_{km}| \le v_{TQ} \le V_m |\sin\theta_{km}| \quad (44)$$

Now, we return to the shunt branch of the UPFC. We consider a constrained control law similar to that used for voltage series components. It is a first order DAE equation written as follows. The reference value is taken proportional to voltage deviation. Because of the slow dynamics of the interface capacitor, here not considered, the time constant τ_Q in (45) is taken lightly greater then τ_V in (40) and (41).

$$\frac{dQ_{sh}}{dt} = \frac{Q_{sh}^{ref} - Q_{sh}}{\tau_Q} \quad (45)$$

$$-Q_{\max} \le Q_{sh} \le Q_{\max} \quad (46)$$

VI. Simulations and comments

The topological structure of the test system is depicted on Fig.7 in Appendix. It is composed by 7 buses connecting 3 transformers, 3 lines, 2 loads, a wind energy generator G1 placed at bus 1 and 2 synchronous machines G2 and G3 placed at buses 6 and 7 respectively. Bus 7 is use as common reference for voltage vectors (slack bus). The UPFC will be place in the line connecting buses 4 and 5. All parameters and data of initial steady state operating point are given in appendix. They are considered in pu with respect to 100 MW power base. All DAEs are solved by PSAT [21] package except models of the UPFC and the wind energy generator. These two models are built separately from PSAT. At each step integration time, we get necessary values of voltages and currents from PSAT and we solve independently these two models. The result is then injected in PSAT and the process continues.

The investigated perturbation scenario includes two parts:

Part 1: The power of the wind generator is set to a constant of 0.5 pu and the UPFC is tested in regulating voltage magnitude of bus 4 at 1.1 pu and in establishing an equivalent series capacitor of 30% of the line reactance. These two commands are injected at t=2 s and the simulation is maintained until t=30 s,

Part 2: At t=30 s, a wind energy variation process described by a ramp of 0.025 pu per second takes place. At t=40 s, the protective system, detecting this high ramp of power evolution, shutdown instantaneously the generator. The response of the UPFC is then observed.

IV.1 Results of Part 1

Table 4 of the Appendix reports initial load flow. It shows that buses 1, 2 and 3 in wind energy generator neighbour have the most low voltage magnitudes. The minimum voltage magnitude is 0.91868 at bus 1. After applying the UPFC device, the voltage level is highly reinforced as reported by Table 5 giving the steady state load flow with constant wind energy value 0.5 pu. The minimum voltage remains at bus 1 but it becomes 1.0371. Table 5 shows also that the final reactive power of the UPFC is about 0.1261 pu which is a reasonable value.

The transient regime is summarized by Fig.8 to Fig.11. We can in particular observe the normal convergence of all variables to their new steady state values. No undesirable oscillation phenomenon is encountered. Note also on Fig.10 that injected active powers of the UPF move in opposite senses. This confirms that the extracted quantity from the input port is absorbed by the series voltage source. However, as shown by Fig.9, the reactive power balance is not null. The reactive power of the input port (Q4) is positive which implies that it is really injected in the bus that works therefore as receiver. In contrary, the output port works as reactive power generator. The final balance is that UPFC furnishes a positive reactive power quantity. It is also to remark that UPFC have effectively realized the function of line reactance compensation. This is confirmed by Fig.11 giving the transited reactive power by the line 4-5. This flow is increased by about 0.3 pu. This quantity is adequate with the value of the parameter η_x considered effectively $\eta_x = 0.3$ in simulation.

IV.1 Results of Part 2

The variable wind energy process of part 2 is shown on Fig.12. The injected power is linearly increased from 0.5 pu (t=30 s) to 0.75 pu (t=40 s). Then, the generator is suddenly tripped. The image of this scenario is clearly present in the dynamic response of the system. Fig.13 depicts the reactive power balance at the two ports of the UPFC. Again, the input port is a reactive power receiver and the output port generates reactive power.

Finally, to definitively confirm that UPFC realizes the designed function parts 1 and 2 of the perturbation scenario are simulated without UPFC. A typical phenomenon of voltage collapse is observed; as depicted by Fig.14. We conclude that the realized control by the UPFC system is very helpful to wind energy penetration in the power system.

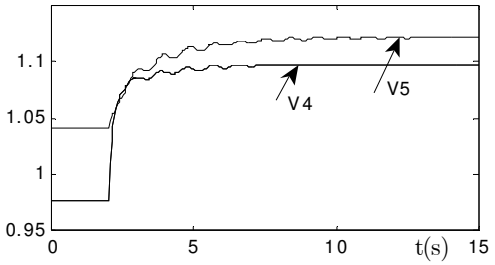

Fig.8 . Dynamic response of V4 and V5 (Part 1)

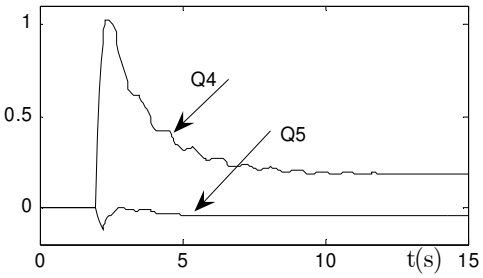

Fig.9 . Dynamic response of Q4 and Q5 (Part 1)

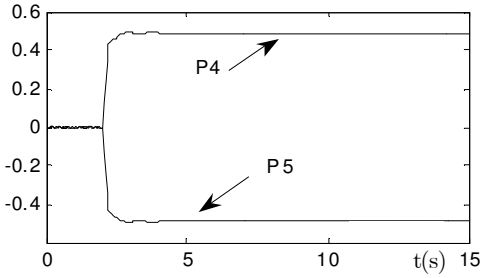

Fig.10 . Dynamic response of P4 and P5 (Part 1)

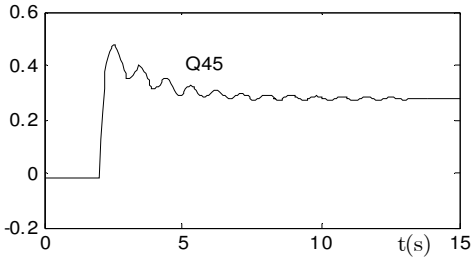

Fig.11 .Response of reactive power of line 4-5 (Part 1)

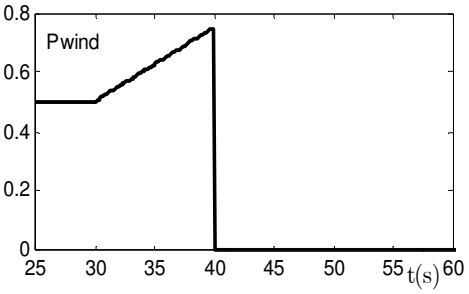

Fig.12. The wind energy variation process (Part 2)

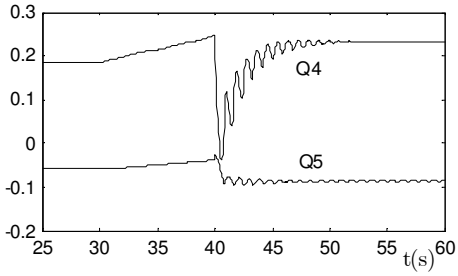

Fig.13 . Dynamic response of Q4 and Q5 (Part 2)

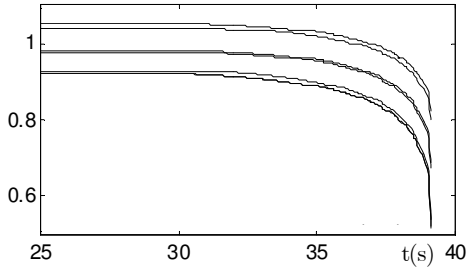

Fig.14. A voltage collapse phenomenon is encountered without UPFC (Part 2)

VII. Conclusion

The main goal of this paper has concerned Unified Power Flow Controller modelling and command. The study is carried out in the context of large power systems including fluctuated power injection such that wind energy generation. Thus, synchronous machine and wind energy source modelling is also integrated. The UPFC model is treated with respect to the principle of power injection equivalent sources. All necessary equations to compute these injections are presented and commented. The study concretized by simulation of a didactic power system.

The simulation of a realistic perturbation scenario is given and commented. Obtained results largely confirm the high capabilities of the UPFC to control voltage level and to compensate a sufficient ratio of the associate energy transmission line. The device works well even in highly variable injected power level. It was shown in particular that UPFC can be a suitable solution against voltage collapse phenomenon.

Appendix

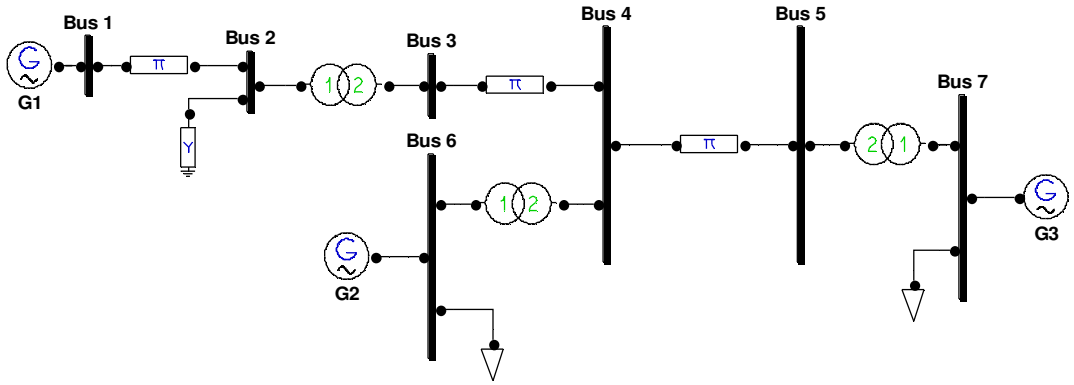

Fig.7.Structure of studied power system

TABLE I
LINES AND TRANSFORMERS REACTANCES

From Bus	To Bus	X(pu)
1	2	0.0302
2	3	0.0500
3	4	0.2000
4	5	0.2000
5	7	0.0125
4	6	0.0167
Shunt(Bus2) : X=5 pu		

TABLE II
UPFC PARAMETERS

$v_{\max} = 0.2$	$Q_{sh\max} = 1$
$\tau_V = 0.1$	$\tau_Q = 0.2$
$\eta_x = 0.3$	$\eta_p = 0.2$

TABLE III
INITIAL STATE AND PARAMETERS OF SYNCHRONOUS MACHINES

	G2	G3
E_d'	0.34673	0.04397
E_q'	1.0362	1.2343
δ_r	1.0468	0.07299
E_{fd}	1.9762	1.8994
P_m	3.2	0.3
X_d	1.59	1.59
X_q	1.36	1.36
X_d'	0.349	0.349
X_q'	0.579	0.579
T_{do}'	2.88	2.88
T_{qo}'	1.08	1.08
D	2	2
H	5	5

Manuscript received November 2008, revised December2008

TABLE IV
INITIAL LOAD FLOW OF THE POWER SYSTEM WITHOUT UPFC

Bus	V(pu)	(°)	PG(pu)	QG(pu)	PL(pu)	QL(pu)
1	0.91868	30.0813	0.5	-	-	-
2	0.91882	29.0548	-	-	-	-
3	0.9289	27.3763	-	-	-	-
4	0.97672	21.0482	-	-	-	-
5	1.0397	1.4872	-	-	-	-
6	0.98	21.9462	3.2	1.2664	2	1
7	1.05	0	0.3	1.6709	2	1

TABLE V
LOAD FLOW OF THE POWER SYSTEM WITH UPFC (PART 1)

Bus	V(pu)	(°)	PG(pu)	QG(pu)	PL(pu)	QL(pu)
1	1.0371	31.8593	0.5	-	-	-
2	1.0372	31.0538	-	-	-	-
3	1.0482	29.7362	-	-	-	-
4	1.0974	24.7492	0.48544	0.18201	-	-
5	1.1205	3.9382	-0.48544	-0.05594	-	-
6	1.1019	25.4594	3.1991	1.4005	2	1
7	1.1296	0	0.30094	1.6295	2	1

References

[1] R. J. Nilson, J. Bian, J. L. Williams "Transmission Series Power Flow Control", IEEE Trans. On Power Delivery, Vol.10, No.1, 1995.

[2] K. R. Padyar, A. M. Kulkarni, "Control Design and Simulation of Unified Power Flow Controlle", IEEE Trans. On Power Delivery, Vol.13, No.4, 1998.

[3] Z. T. Faur, " Effects of FACTS devices on static voltage collapse phenomen", Thesis of University of Waterloo, Ontario, Canada, 1996.

[4] Kalyan K. Sen, Eric J. Stacey, "UPFC: Unified Power Flow Controller: Theory, Modelling and Applications", IEEE Trans. On Power Delivery, Vol.13, No.4, 1998.

[5] P. W. Lehn, M. R. Iravani, "Experimental Evaluation of STATCOM Closed Loop Dynamics", IEEE Trans. On Power Delivery, Vol.13, No.4, 1998.

[6] Claudio A. Canizares, Zeno T. Faur, "Analysis of SVC and TCSC Controllers in Voltage Collapse", IEEE Trans. On Power Delivery, Vol.14, No.1, 1999.

[7] Paolo Mattavelli, Aleksandar M. Stankovik, Georges C. Verghese, "SSR Analysis with Dynamic Phasor of Thyristor-Controled Series Capacitor", IEEE Trans. On Power Delivery, Vol.14, No.1, 1999.

[8] H. F. Wang, "Damping function of unified power flow controller", IEE Proc. Gener. Transm. Distrib. Vol.146, No.1, 1999.

[9] M. Ghandhari, "Control Lyapunov function: A control strategy for damping of power oscillations in large power systems", Thesis of the Royal Institute of Technology, Stockholm, Sweden, 2000.

[10] L. Angquist, "Synchronous voltage reversal control of thyristor controlled series capacitor", Thesis of the Royal Institute of Technology, Stockholm, Sweden, 2002.

[11] N. Mithulananthan, " Power system with interacting generator and FACTS controllers", Thesis of University of Waterloo, Ontario, Canada, 2002.

[12] M. Januszewski, J. Machowski, J. W. Bialek, "Application of the direct Lyapunov method to improve damping of power swings by control of UPFC", IEE Proc.Gener. Transm. Distrib. Vol.151, No.2, March 2004.

[13] R. E. Mahony, L. M. Mareels, " Global solution for differential/algebraic systems with implications for Lyapunov direct stability methods", Journal of Mathematical Systems, Estimation and Control, Vol.5, No.4, 1995.

[14] R. Dhifaoui, H. Brahmi, O. Hasnaoui, F. Bacha, "Investigation of the unstable orbit of fourth order model of one machine infinite bus system", GESTS Int. Trans. On Computer Science and Engineering, Vol.26, No.1, 2006

[15] J. Marques, H. Pinheiro, H. A. Grundling, J. R. Pinheiro, H. L. Hey, "A survey on variable speed wind turbine system", in Congresso Braseleiro de Electronica de Potencia, (COBEP), 2003, Fortalesa-CE Brazil

[16] V. Akhmatov, H. Knudsen, A. H. Nilson, J. K. Pederson, N. K. Poulsen, "Modelling and transient stability of large wind farms", Electrical power and energy system 25, Elsevier science 2003.

[17] V. Akhmatov, H. Knudsen, A. H. Nilson, J. K. Pederson, N. K. Poulsen, "Modelling and transient stability of large wind farms", Electrical power and energy system 25, Elsevier 2003.

[18] P. Ledesma, J. Usaola, J. L. Rodriguez, "Transient stability of fixed speed wind", Renewable energy 28, Elsevier 2003.

[19] Hasnaoui Othman, Inès Ben Salem, Mohamed Faouzi Mimouni, Dhifaoui Rachid, " Modelling and Control of a Variable Speed Wind Energy Conversion Turbine driven Synchronous Generator Connected to the Grid", WSEAS Transactions on Systems, Issue 6, Vol. N°.5, ISSN 1109-2777, pp. 1257-1264, Juin 2006

[20] Inès Ben Salem, Hasnaoui Othman, Dhifaoui Rachid, "Control of Direct Drive Synchronous Generator for Wind Energy Conversion Systems", JTEA'06, Hammamet, Tunisie.

[21] M'Hamdi Gharbia, , Wergui Ammar, Hasnaoui Othman, Dhifaoui Rachid, "Sur la modélisation et la commande d'éolienne à machine asynchrone doublement alimentée", Sixième conférence Internationale des Sciences et Techniques de l'Automatique STA'05, Décembre 2005, Sousse, Tunisie

[22] Federico Milano, "An Open Source Power System Analysis Toolbox", IEEE Trans. On Power Systems, Vol.20, No.3, 2005.

Authors' information

Houda Brahmi is born in Tunis, Tunisia 1978. She obtained the engineer diploma of engineer and the master diploma in Industrial Informatics and Automatics from (INSAT), Tunisia, respectively in 2003 and 2004. She is an associate Professor at Manar University (ISTMT) and her field of interest concerns the Electrical Machines and Power Systems.

Post address: INSAT– Centre Urbain Nord – Rue de la Terre- BP 676 – 1080 Tunis Cedex Fax : 216-71-704-329
e-mail : houda.brahmi@yahoo.fr

Rachid Dhifaoui is born in Kairouan, Tunisia'1954. He received "Doctorat d'Etat" in Electrical Engineering from ENSET, University of Tunis II, 1991. He is now permanent professor at National Institute of Applied Sciences and Technology (INSAT). He manages the studies of a Master Cycle in Industrial Informatics and Automatic Control. He is a manager of a research group (RME) working in the field of Electrical Machines and Power Systems.

Post address: INSAT– Centre Urbain Nord – Rue de la Terre- BP 676 – 1080 Tunis Cedex Fax : 216-71-704-329
e-mail : Rachid.Dhifaoui@insat.rnu.tn

